Functional Cationic Nanomagnet – Porphyrin Hybrids for the Photoinactivation of Microorganisms

ARTICLE *in* ACS NANO · DECEMBER 2010

Impact Factor: 12.88 · DOI: 10.1021/nn1026092 · Source: PubMed

12 AUTHORS, INCLUDING:

Carla Marisa Brito Carvalho
University of Aveiro
22 PUBLICATIONS **526** CITATIONS
SEE PROFILE

Maria Faustino
University of Aveiro
152 PUBLICATIONS **1,659** CITATIONS
SEE PROFILE

Zhi Lin
University of Aveiro
130 PUBLICATIONS **1,645** CITATIONS
SEE PROFILE

Sonia L C Pinho
University of Coimbra & Biocant
111 PUBLICATIONS **1,642** CITATIONS
SEE PROFILE

Functional Cationic Nanomagnet–Porphyrin Hybrids for the Photoinactivation of Microorganisms

Carla M. B. Carvalho,[†] Eliana Alves,[‡] Liliana Costa,[‡] João P. C. Tomé,[†] Maria A. F. Faustino,[†] Maria G. P. M. S. Neves,[†] Augusto C. Tomé,[†] José A. S. Cavaleiro,[†,*] Adelaide Almeida,[‡] Ângela Cunha,[‡] Zhi Lin,[§] and João Rocha[§]

[†]QOPNA/Department of Chemistry, [‡]CESAM/Department of Biology, and [§]CICECO/Department of Chemistry, University of Aveiro, 3810-193 Aveiro, Portugal

ABSTRACT Cationic nanomagnet–porphyrin hybrids were synthesized and their photodynamic therapy capabilities were investigated against the Gram (−) *Escherichia coli* bacteria, the Gram (+) *Enterococcus faecalis* bacteria and T4-like phage. The synthesis, structural characterization, photophysical properties, and antimicrobial activity of these new materials are discussed. The results show that these new multicharged nanomagnet–porphyrin hybrids are very stable in water and highly effective in the photoinactivation of bacteria and phages. Their remarkable antimicrobial activity, associated with their easy recovery, just by applying a magnetic field, makes these materials novel photosensitizers for water or wastewater disinfection.

KEYWORDS: porphyrins · cationic · nanomagnets · photoinactivation · microorganisms · hybrid materials

Photodynamic therapy (PDT) is a technique where undesirable cells or tissues (*e.g.*, pathogenic microorganisms or tumors) are destroyed by reactive oxygen species, mainly singlet oxygen, generated by a photosensitizer (PS) upon irradiation with visible light in the presence of oxygen.[1,2] Studies performed with porphyrin-based photosensitizers point out the great potentiality of this type of compounds for biomedical applications, namely for treatment of oncological, cardiovascular, dermatological, and ophthalmic diseases.[3] Recent studies demonstrated that PDT can be also very effective in the photoinactivation of microorganisms (MO) and can become a potential alternative for the treatment and eradication of emerging bacterial strains resistant to antibiotics, viruses resistant to classical antiviral drugs, fungi, and protozoa.[4−6] Moreover, some researchers are investigating the possibility of using this technique not only for application in the clinic field but also in environmental applications, more specifically for the inactivation of pathogenic MO in water and wastewater.[7−9]

Although the transmission of microbial diseases seems to be highly reduced, at least in developed countries, by the improvement of water supplies and hygienic-based procedures for a whole range of human activities, it is recognized that new environmentally friendly technologies are needed for combating microbial contamination in water and wastewater.[10]

Recent works have shown that cationic porphyrin derivatives can efficiently photoinactivate both Gram (+) and Gram (−) bacteria types, even without the presence of membrane disrupting agents (*e.g.*, $CaCl_2$, EDTA or polymixin B nonapeptide). These results are important, especially due to the resistance of Gram (−) bacteria to the direct action of neutral and anionic PS without the presence of those membrane disrupting agents.[4,6,11] However, the extension of the photodynamic principle to a new environmentally friendly technology can only become economically viable if the PS is immobilized on a solid matrix in order to allow its complete recovery after the photoinactivation process. Few studies have explored this approach. Bonnett *et al.*[12] reported the immobilization of *meso*-tetraarylporphyrins with amino and hydroxy substituents by adsorption into chitosan, and also a phthalocyanine tetrasulfonic acid by covalent attachment. The photomicrobicidal evaluation of these systems showed that the most effective is the one where the PS is covalently attached to the polymer.

In recent years we have been developing efficient photosensitizers for the photoinactivation of environmental MO. Having in mind their recovery and reuse, we considered the possibility of immobilizing those PS on magnetic nanoparticles.[13] The use of magnetic nanoparticles as a template for the dispersion of a PS can facilitate its recovery in a wastewater treatment plant just by

*Address correspondence to jcavaleiro@ua.pt.

Received for review June 2, 2010 and accepted November 12, 2010.

10.1021/nn1026092

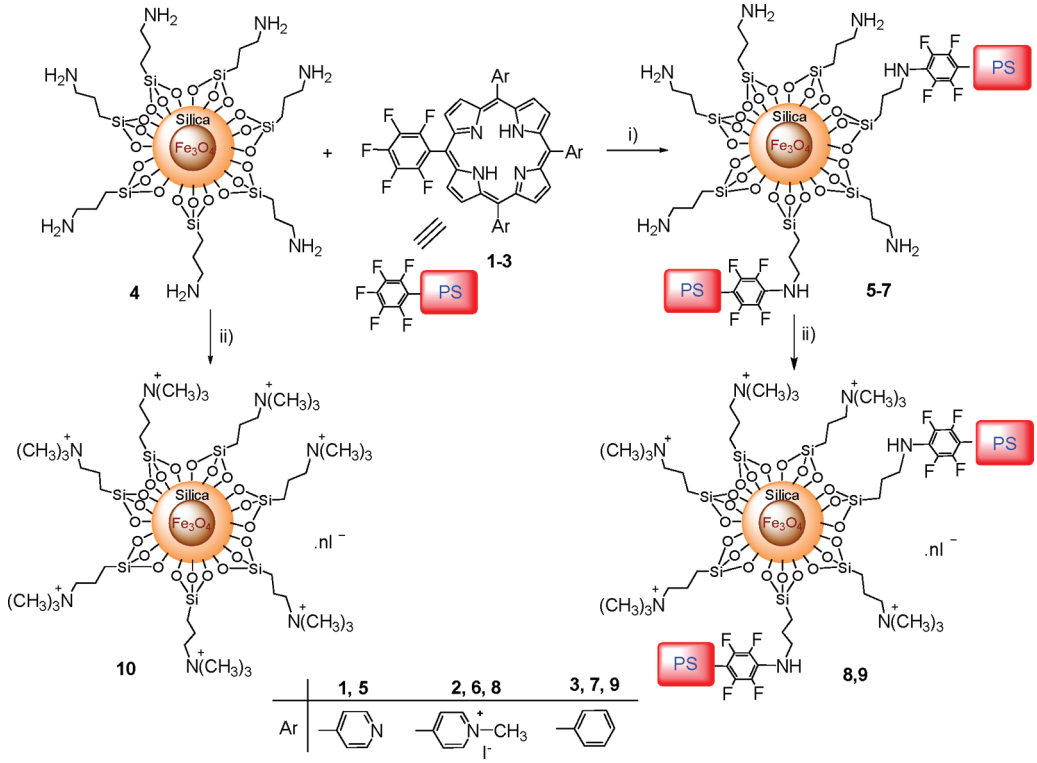

Scheme 1. Synthesis of the nanomagnet−porphyrin hybrids 5−9 and the cationic nanomaterial 10. Conditions: (i) DMSO, 140 °C, 24 h; (ii) CH_3I, DMF, 40 °C, overnight.

applying a magnetic field.[14,15] Nanoparticles with magnetic characteristics have been widely used in biology and medicine for protein and enzyme immobilization,[16] immunoassays,[17] DNA purification,[18] cell isolation[19] and drug delivery.[20,21] However, to the best of our knowledge, this is the first time that magnetic nanoparticles functionalized with neutral and cationic porphyrins are used as antimicrobial materials.

RESULTS AND DISCUSSION

The synthetic route to the novel magnetic nanoparticle−porphyrin conjugates **5**−**9** is shown in Scheme 1. The starting magnetic template **4**[22] and the porphyrins used in this work [5-(pentafluorophenyl)-10,15,20-tris(4-pyridyl)porphyrin (**1**), 5-(pentafluorophenyl)-10,15,20-tris(1-methylpyridinium-4-yl)porphyrin tri-iodide (**2**) and 5-(pentafluorophenyl)-10,15,20-triphenylporphyrin (**3**) were prepared according to the literature, with minor modifications.[23] The grafting of porphyrins **1**, **2**, and **3** on the magnetic nanomaterial **4** was carried out in DMSO at 140 °C. After 24 h, TLC of each reaction mixture showed that most of the starting porphyrin was converted into a new red-colored material that remains in the baseline. The resulting solids were filtered and washed with the appropriate solvent in order to remove the residual unbound porphyrin. This process was monitored by UV−vis and stopped when no Soret band was detected in the rinse solvent (Supporting Information, Figure S1). The amount of porphyrin covalently bound to the nanomaterial was calculated by subtracting the amount of recovered porphyrin in the combined washing solvents (measured by UV−vis) to the initial amount of porphyrin used. In the three materials **5**−**7**, the relative amount of porphyrin is *ca.* 4−5% (w/w).

The neutral hybrids **5** and **7**, when suspended in water, show a high tendency to aggregate. However, the suspensions of the cationic material **6** in water showed a reasonable stability (Figure 1a), probably due to charge repulsion between each individual particle. So, in order to circumvent this situation, we decided to quaternize the free amino groups of the new materials **5**−**7** and also the magnetic nanomaterial **4**; this one to be used as control in the biological assays (Scheme 1). The cationization process was carried out with a large excess of methyl iodide in DMF at 40 °C.[11] After 16 h, the cationic hybrids **8** and **9**, and the cationic nanomaterial **10**, were filtered and thoroughly washed with water. After the cationization, materials **5** and **6** give ex-

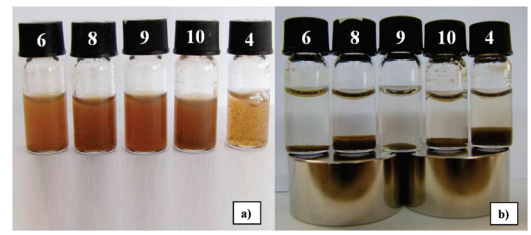

Figure 1. Water suspensions of the magnetic materials 4, 6, 8−10; (a) in the absence of a magnetic field, (b) in the presence of a magnetic field.

actly the same material **8**, since the pyridyl groups of **5** are also methylated.

Hybrids **6** and **8** are constituted by the cationic porphyrin **2** coupled, respectively, to the neutral or cationized nanomaterial **4**. Hybrid **9** is constituted by the neutral porphyrin **3** coupled to cationic nanomaterial. Our previous results, on the bactericidal effect of porphyrins with different number and distribution of positive charges and different *meso*-substituent groups, led us to consider porphyrin **2** to construct hybrids **6** and **8**.[24,25] This porphyrin showed to be the most efficient PS against *Enterococcus faecalis* (*E. faecalis*) and *Escherichia coli* (*E. coli*) strains and also against a bioluminescent recombinant *E. coli* strain, other faecal coliforms, sewage bacteriophages, and bacterial endospores.[25−27] Porphyrin **3** was chosen to build hybrid **9** in order to check if the presence of positive charges in the porphyrin macrocycle is an essential feature for the efficiency of the hybrid nanomaterials. It is worth noting that both porphyrins **2** and **3** have a pentafluorophenyl group that allowed the covalent linkage to the nanomagnet **4**.

As expected, water suspensions of the new cationic materials show a minor tendency to form clusters/aggregates more so than the suspensions of the corresponding precursors **5**−**7** (Figure 1a). That is due to a higher repulsion between the nanoparticles caused by the increased number of positive charges. In this respect, suspensions of hybrid **8** proved to be the most stable ones.

Figure 1a shows water suspensions of cationic hybrids **6**, **8**, and **9**, that can be stirred on a magnetic plate even without a magnetic stirrer. Figure 1b shows the deposition of the same materials, which occurs in a few seconds when placed on the top of two small supermagnetic discs. This behavior confirms that the material can be easily recovered, just by using the influence of a permanent magnetic field.

All the cationic nanomagnet−porphyrin hybrids were characterized by powder X-ray diffraction (XRD), transmission electron microscopy (TEM), selected area electron diffraction (SAED), and solid-state UV−vis spectrophotometry.

Powder XRD was performed in the range 10−90° 2θ on a Philips X'pert MPD diffractometer using Cu Kα radiation. The pattern shown in Supporting Information, Figure S2 is from a nanosupport sample, which was kept in ethanol for more than 1 year. Magnetite (Fe_3O_4) is the main crystal phase present, the sample being black. Small amounts of maghemite cannot be discarded, since both magnetite and maghemite have a spinel structure and exhibit very similar powder XRD patterns. However, maghemite is brown in color, not black. The peak at 44.65° 2θ probably results from α-Fe metal while the broad peak at *ca.* 28° 2θ is ascribed to the amorphous SiO_2 shell. This indicates that the nanosupport is stable. The crystallite size may be estimated

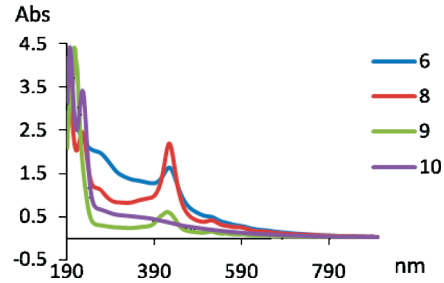

Figure 2. Solid-state UV−vis spectra of the hybrids 6, 8, and 9 and material 10.

via the full-width at half-maximum (fwhm) of the strongest XRD reflection, using the well-known Scherrer formula.[28] Using the peak at 35.56° in Supporting Information, Figure S2, the crystallite size of magnetite is estimated to be *ca.* 18 nm. This result is in accordance with TEM evidence (Supporting Information, Figure S3).

TEM images and SAED patterns were recorded on a Hitachi H9000 NA microscope operated at 200 kV. Supporting Information, Figure S3 shows a TEM image of an assembly of cationic nanomagnet−porphyrin hybrid nanoparticles with an average size of *ca.* 20 nm (including the SiO_2 shell). The SAED pattern of the cationic nanomagnet−porphyrin hybrid nanoparticles (Supporting Information, Figure S4), reveals that the nanosupport remains crystalline after the surface immobilization of porphyrin.

The UV−vis spectra of the hybrid materials **6**, **8**, and **9** and of material **10** are shown in Figure 2. The characteristic Soret band of a porphyrin derivative (at *ca.* 400 nm) in the hybrid spectra indicates clearly the success of the immobilization process and the preservation of the structural features of the PS.

The photostability of the nanomaterials **6**, **8**, and **9** was evaluated under the same conditions used in the biological assays (white light, 380−700 nm, 40 W m^{-2}). This parameter was calculated by the ratio of the residual absorbance (measured at the Soret band) before and after irradiation for different periods of time. Under these conditions, all the cationic hybrids show suspension stability (dark control) and photostability, as exemplified in Figure 3 for material **8**. Materials **6** and **9** show a small absorbance decrease similar to that observed in the dark, probably due to aggregation phenomena (Supporting Information, Figure S5). The nonimmobilized porphyrins **2** and **3** have also been described as photostable under similar irradiation conditions. The nonphotobleaching of the materials indicates that no extensive destruction of the porphyrin macrocycle occurs. This is an important parameter that certifies that the recycled material will be operational for a long time.

To evaluate the potentiality of the new hybrids in the photodynamic inactivation of MO, their capacities to generate singlet oxygen were estimated qualitatively using 1,3-diphenylisobenzofuran (DPiBF) as a $^1O_2$ indi-

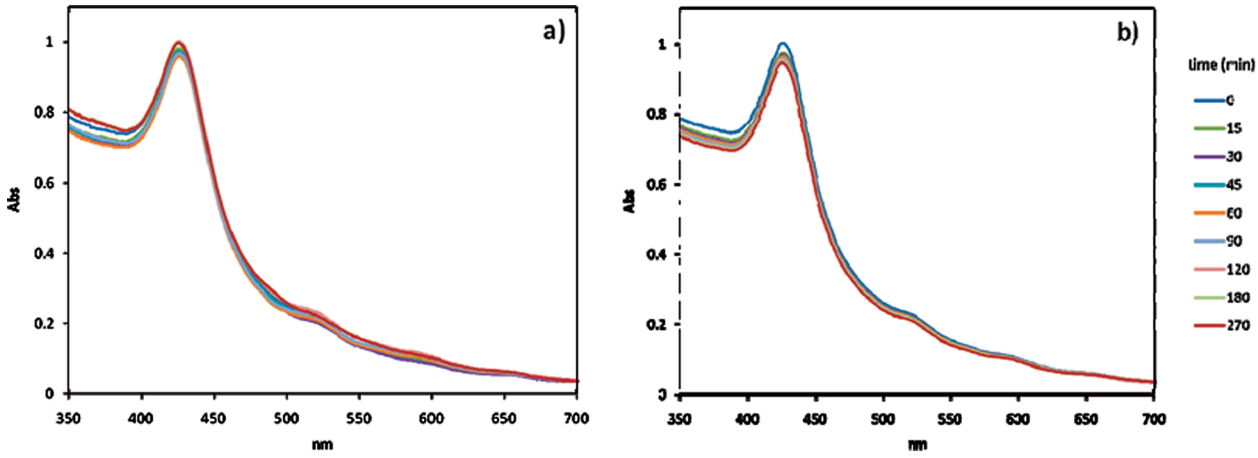

Figure 3. Photostability and stability of a water suspension of 8: (a) after irradiation with white light (40 W cm^{-2}) for different periods of time; (b) stability in solution (without irradiation).

cator. The yellow DPiBF reacts with $^1O_2$ in a [4 + 2] cycloaddition being oxidized to colorless *o*-dibenzoylbenzene. Since DPiBF has an absorption maximum at 415 nm, it is possible to follow the ability of the PS to generate $^1O_2$ by measuring the absorption decay, at this wavelength. A DMF/H_2O (90:10) solution of DPiBF and the PS was irradiated with white light filtered through a cutoff filter for wavelengths <540 nm (40 W m^{-2}). The results summarized in Figure 4 show that the new hybrids **6**, **8**, and **9**, at 20 μM, are able to generate singlet oxygen at a rate similar to that of the nonimmobilized porphyrins **2** and **3** at 0.5 μM. No significant differences were observed among the three nanomaterials.

To be used as disinfectants in a wastewater treatment plant, the nanomagnetic−porphyrin hybrids should be able to efficiently photoinactivate a broad spectrum of MO. To test if the synthesized hybrids meet this requirement, the antimicrobial efficiencies of the three cationic hybrids **6**, **8**, and **9** were tested against the Gram (−) *E. coli*, the Gram (+) *E. faecalis* bacteria,

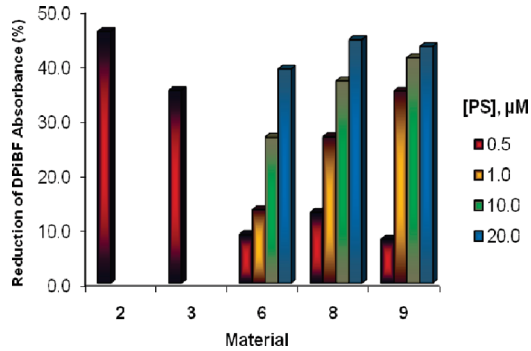

Figure 4. Reduction of DPiBF absorbance in the presence of the nonimmobilized porphyrins 2 and 3 or the target PS 6, 8, and 9 at different concentrations after 10 min of irradiation with white light filtered through a cutoff filter for wavelengths <540 nm (40 W m^{-2}). Concentrations indicated for the nanomaterials 6, 8, and 9 refer to the equivalent concentration of nonimmobilized porphyrins. Each point represents the mean of two independent experiments, with two replicates each, and has a standard deviation lower than 5%.

and also T4-like phage. The selected bacteria and the T4-like phages are commonly used as indicators of the presence of pathogenic MO in wastewaters. The phototoxicity of the various PS was determined using both bacterial and phage suspensions in phosphate buffered saline (pH ≈ 7.4) with appropriate concentration of PS, followed by irradiation with white light, at a fluence rate of 40 W m^{-2} for 270 min (total light dose of 64.8 J cm^{-2}). The efficiency of bacterial and viral photoinactivation by the various PS was evaluated through quantification of the number of MO in laboratory conditions, before and after light exposition, using bacterial suspensions with ~5 log CFU mL^{-1} and phage suspensions with ~7 log PFU mL^{-1}. For each PS two independent experiments were done, and the results shown are the average of two assays.

Four controls were carried out: (i) dark toxicity control (MO exposed to PS without irradiation); (ii) light control (MO exposed to irradiation without PS); (iii) nonimmobilized porphyrin control (MO exposed to derivative **2** under irradiation); and (iv) support control (MO exposed to the cationic magnetic silica nanoparticles **10** under irradiation). No considerable decrease in cell survival was observed upon dark incubation with all target PS and upon irradiation without PS or in the presence of the neutral (**4**) or cationic (**10**) support nanomaterials.

The results of the photoinactivation of the Gram (−) *E. coli* and T4-like phage by photosensitizers **2**, **6**, **8**, and **9** are summarized in Table 1.

For all tested hybrids (**6**, **8**, and **9**) it is necessary to use a higher concentration of immobilized PS to get a photoinactivation similar to that observed with the free PS (Supporting Information, Figure S7), as expected from the results of singlet oxygen generation (Figure 4). For example, with porphyrin **2** a concentration of 5 μM and a light dose of 21.6 J cm^{-2} is sufficient to get a nearly total photoinactivation of *E. coli* (4.8 log). However, to get approximately the same result with hybrid **6**, at the same light dose, the PS concentration on the

TABLE 1. PS Minimum Concentration (μM) *versus* Light Dose (J cm^{-2}) Causing the Highest Decrease in the Survival (log) of the Selected Microorganism upon White Light Irradiation at a Fluence Rate of 40 W m^{-2}

	E. coli[a]			T4-like phage[b]		
PS	[PS] (μM)	light dose (J cm^{-2})	survival decrease (log)	[PS] (μM)	light dose (J cm^{-2})	survival decrease (log)
2	5	21.6	4.8[c]	5	43.2	6.9[c]
6	200	21.6	4.7[c]	20	64.8	6.9[c]
8	20	43.2	4.8[c]	20	14.4	6.8[c]
9	200	64.8	0.2	100	64.8	5.2

[a]Initial concentration = 10^5 CFU mL^{-1}. [b]Initial concentration = 10^7 PFU mL^{-1}. [c]Detection limit.

material must be 200 μM. With material **8** a concentration of 20 μM and a light dose of 43.2 J cm^{-2} is required to obtain a similar photoinactivation. Hybrid **9** is clearly the weakest PS against *E. coli*. Even at 200 μM, and a light dose of 64.8 J cm^{-2}, it leads to a reduction of only 0.2 log on cell viability.

It is well-known that Gram (+) bacteria are easily photoinactivated, not only with cationic PS but also with neutral and anionic ones, due to their membrane higher permeability.[6] Our studies confirm this observation since all tested hybrids (**6**, **8**, and **9**) induced a total photoinactivation of *E. faecalis*, *ca.* 5.0 log drop on cell viability (data not shown), even when used at 20 μM and after a light dose of 21.6 J cm^{-2} (90 min of irradiation).

The three cationic hybrids were also evaluated against T4-like phage and all showed to be very efficient against nonenveloped viruses (Table 1 and Supporting Information, Figure S8). The best materials, **6** and **8**, are able to induce a complete photoinactivation of T4-like phage (6.9 log) at 20 μM, after a light dose of 64.8 and 14.4 J cm^{-2}, respectively.

The biological results showed that hybrid **8** (cationic PS coupled to cationic material) at 20 μM was the most effective material against both Gram bacteria types and T4-like phage, where a light dose of 43.2 and 14.4 J cm^{-2}, respectively, was only necessary for complete photoinactivation. Hybrid **6** (cationic PS coupled to neutral material) was the second most effective one showing, at the same PS concentration, a similar photoinactivation for *E. faecalis* and T4-like phage, but for the last one a higher light dose (64.8 J cm^{-2}) is required. To attain a similar efficiency against *E. coli* a much higher concentration is required. Hybrid **9** (neutral PS coupled to cationic material) is clearly the less efficient material. It is effective against *E. faecalis* but not against *E. coli*.

Comparing the results obtained with hybrid **8** and hybrid **9**, it is evident that positive charges in the PS are essential to achieve a significant photoinactivation of *E. coli*. The positive charges in the nanomaterial play other important roles, such as the stabilization of the magnetic nanoparticles in water suspensions, allowing a higher availability of the PS for the photodynamic process.

Phthalocyanines immobilized on chitosan matrices[12] were considered good PS for the photodisinfection of polluted waters with microbial levels lower than those tested in this work. However, only a maximum of 2.25 log kill was achieved.[12] In our study, for the same initial bacterial level, a 5 log cell kill was attained with the best hybrids. Both **6** and **8** can be considered excellent bactericidal hybrids since they can promote the photoinactivation of the tested strains even at higher levels than those typically present in contaminated waters. Furthermore, the complete photoinactivation of T4-like phage by these two nanomaterials suggests that they might be able to photoinactivate a large spectrum of MO. It is worth noting that the artificial light fluence (40 W m^{-2}) used in this study for the photoinactivation of both bacteria and phage is much lower than solar visible radiation (400−700 nm). In temperate climates, as in Portugal, where this work was carried out, solar visible radiation reaches fluence rates of about 400 W m^{-2} in winter and 620 W m^{-2} in summer. This means that if sunlight is used as the light source, the time needed for an efficient photodynamic process will be much shorter than the 4.5 h required in this study.[29] Therefore, the use of this technology for wastewater treatment under natural light conditions may be a simple, not expensive, and accessible process. Additionally, the magnetic nanoparticles have the following advantages: the magnetic core of iron oxide allows the removal of the PS from the surrounding medium (essential for the recovery and reuse of the antimicrobial hybrids) and the silica coating avoids the oxidation, and consequent degradation, of the magnetic core; it is also useful to prevent the aggregation and partial exposure of naked magnetite.

CONCLUSIONS

The novel cationic nanomagnet−porphyrin hybrids can be considered highly efficient for the photoinactivation of bacteria and phages. Hybrid **8** turned out to be the most effective material: at 20 μM it caused a total photoinactivation (to the limit of detection) of *E. faecalis*, *E. coli*, and T4-like phage, upon irradiation with white light of 21.6, 43.2, and 14.4 J cm^{-2}, respectively. With these results we can anticipate that it should have a broad action spectrum against bacteria and viruses and may be used to disinfect water or wastewater. In addition, this magnetic material can be easily recovered

from the treated systems just by applying a magnetic field.

Currently we are testing hybrid **8** under different meteorological conditions of light and temperature in order to evaluate its reuse on large scale microbial photoinactivation. The use of magnetic template **4** to support other types of PS, eventually cheaper than porphyrins, is also under evaluation.

EXPERIMENTAL SECTION

Synthesis of Porphyrins 1−3. Neutral porphyrins **1** and **3** were synthesized by the crossed Rothemund reactions using pyrrole and the adequate benzaldehydes (pentafluorobenzaldehyde and pyridine-4-carbaldehyde or benzaldehyde) at reflux in acetic acid and nitrobenzene.[11,23] The resulting compounds were separated and purified by column chromatography (silica). Cationic porphyrin **2** was prepared by quarternization of the three pyridyl groups of porphyrin **1** with methyl iodide. The resulting product was purified by crystallization from water/acetone. The purity of the three porphyrins was confirmed by thin layer chromatography and by ^{1}H NMR spectroscopy, and the spectroscopic data were in accordance with literature.[30] Porphyrin **1**. UV−vis ($CHCl_3$), λ_{max} (log ε): 416 (5.73), 510 (4.33), 542 (3.61), 584 (3.79), 639 (3.19) nm. Porphyrin **2**. UV−vis (DMSO), λ_{max} (log ε): 422 (5.48), 485 (3.85), 513 (4.30), 545 (3.70), 640 (3.14) nm. Porphyrin **3**. UV−vis ($CHCl_3$), λ_{max} (log ε): 417 (5.74), 513 (4.33), 547 (3.81), 588 (3.79), 645 (3.52) nm.

Synthesis of the Magnetic Silica Nanoparticles. The magnetic nanomaterial **4** was prepared according to the literature with minor modifications.[22] The Fe_3O_4 core was obtained by the conventional coprecipitation method with some modifications. $FeNH_4(SO_4)_2$ (2.95 g) and $(NH_4)_2Fe(SO_4)_2$ (1.20 g) were dissolved in deionized water (100 mL) with vigorous stirring at 80 °C. $NH_3 \cdot H_2O$ 25% (3.5 mL) was then added dropwise to the solution. The color of the bulk solution immediately changed from orange to black. The magnetite precipitate was washed twice with deionized water. Sodium metasilicate (23.75 g) was dissolved in deionized water, and the pH value of the solution was adjusted to *ca.* 12 by the addition of a required amount of concentrated hydrochloric acid (37%). The sodium metasilicate solution and the prepared Fe_3O_4 nanocores were poured into a beaker equipped with a mechanical stirrer. The mixture was ultrasonicated for 30 min. Then, the temperature of the mixture was increased to 80 °C. HCl was added dropwise to adjust the pH value to 6−7. The precipitate was washed several times with deionized water and then dispersed in ethanol (800 mL). (3-Aminopropyl)triethoxysilane (APTS) was added to the suspension and the resulting mixture was magnetically stirred at room temperature for 24 h. The precipitate was washed several times with ethanol, and the magnetic nanoparticles were purified by magnetic decantation and then dispersed in the same solvent (600 mL).

Synthesis of the Nanomagnet−Porphyrin Hybrids—Standard Procedure. Recently prepared magnetic silica nanoparticles **4** were filtered through a polyamide membrane; then 500 mg of **4** (743 μmol of aminopropyl groups, 20 equiv) were resuspended in DMSO (1 mL). A solution of each porphyrin **1**−**3** (37.3 μmol) in DMSO (9 mL) was added to that suspension and the resulting mixture was magnetically stirred during 24 h at 140 °C. In each case a red insoluble product (**5**−**7**) was obtained. The immobilization of porphyrin **1**−**3** was monitored by TLC. The resulting hybrid materials were washed with the appropriate solvent (50 mL) (Supporting Information, Table S1) until no Soret band was observed in the rinse solvent (Figure S2, example given for hybrid **6**). In the washing process the materials were decanted by using a magnetic disk. The amount of unreacted porphyrin was calculated by UV−vis spectrophotometry (the ε value at the Soret band, for each porphyrin, is indicated above). Derivative **6** was resuspended in water (50 mL) for the direct evaluation of the antimicrobial activity. The hybrid products were also resuspended in dry DMF (20 mL) for subsequent treatment with methyl iodide. The cationization procedure was carried out by the addition of a large excess of methyl iodide (4 mL) to suspensions of hybrid **5**−**7** in dry DMF (20 mL). The reaction mixtures were kept under stirring at 40 °C for 16 h. After this period the suspensions were cooled down in ice and the cationic hybrids **8** and **9** were filtered and washed up with water (5 × 50 mL). These products were also resuspended in water (50 mL) for antimicrobial activity determination.

Photostability and Stability of Hybrids 6, 8, and 9 in Suspension. The photostability of the hybrids **6**, **8**, and **9** were evaluated by exposing aerated suspensions of these compounds to visible light. In a glass cell, 30 μL of hybrid compound suspensions were diluted in 2 mL of H_2O and were irradiated using the same conditions as in the biological assays (white light, fluence rate of 40 W m^{-2}). During irradiation the suspensions were magnetically stirred, using just the magnetic field of the particles (without a magnetic bar) at room temperature. The UV−vis spectra of these suspensions were recorded at different times of irradiation (0−270 min). To evaluate the stability of the hybrid compounds suspensions, a procedure similar to that described above was followed but now without irradiation (glass cells were kept in the dark).

Determination of the Singlet Oxygen Generation. Stock solutions/suspensions of each PS at 0.1 mM in DMF/water (9:1) (for the hybrid compounds 0.1 mM corresponds to the equivalent concentration of the supported porphyrin) and a stock solution of 1,3-diphenylisobenzofuran (DPiBF) at 10 mM in DMSO were prepared. A mixture of 50 μM of DPiBF and 0.5 μM of a PS derivative in DMF water (9:1) in glass cells (2 mL) was irradiated with white light filtered through a cutoff filter of wavelength < 540 nm, at a fluence rate of 40 W m^{-2}. For the cationic immobilized PS (**6**, **8**, and **9**) the same strategy was followed but PS concentrations of 5, 10, and 20 μM were also used. During the irradiation period, the solutions/suspensions were stirred at room temperature. The generation of singlet oxygen was followed by its reaction with DPiBF. The breakdown of DPiBF was monitored by measuring the decreasing of the absorbance at 415 nm at irradiation intervals of 1 min for 10 min.

Experimental Setup for the Photoinactivation of Bacteria. ***Irradiation Conditions.*** All samples were exposed, in parallel, to white light (PAR radiation, 13 OSRAM 21 lamps of 18 W each, 380−700 nm) with a fluence rate of 40 W m^{-2} (measured with a light meter LI-COR model LI-250, Li-Cor Inc., USA), at 20−25 °C for 270 min, under 100 rpm mechanical stirring. The emission spectrum of white light source used in this study is shown in Supporting Information, Figure S6.

Microorganisms and Growth Conditions. The Gram (−) strain *Escherichia coli* ATCC 13706 and the Gram (+) strain *Enterococcus faecalis* ATCC 29212 were stored at 4 °C in triptic soy agar (TSA, Merck). Before each assay the strains were grown aerobically for 24 h at 37 °C in 30 mL of triptic soy broth (TSB, Merck). Then, an aliquot of this culture (200 μL) was aseptically subcultured into 30 mL of fresh TSB medium and grew overnight at 37 °C to reach an optical density (OD_{600}) of ∼1.3, corresponding to ∼10^8 cells mL^{-1}.

Bacterial Photoinactivation Method. The efficiency of hybrids **6**, **8**, and **9** was assessed using bacterial suspensions. Bacterial cultures of *E. coli* grown overnight ($OD_{600} \approx 1.3$) were diluted one thousand fold in phosphate buffered saline (PBS, pH = 7.4), to a final concentration of ∼10^5 colony forming units (CFU) per mL and equally distributed in 600 mL acid-washed and sterilized glass beakers (20 mL of bacterial suspension in each beaker). Meanwhile, the different hybrids (**6**, **8**, and **9**) were sonicated for 45 min to promote a better disaggregation of the materials. After the addition of bacterial suspension to the beakers, the hybrids were added to the respective beaker until the final concentrations of 20 μM and 200 μM (PS concentration) were achieved.

Four controls were carried out in the same conditions: dark control (MO exposed to PS without irradiation), light control (MO exposed to irradiation without PS), nonimmobilized porphyrin control (MO exposed to **2** (5 μM) under irradiation), and sup-

port control (MO exposed to nanoparticles **4** and **10** under irradiation). The beakers were then exposed to white light radiation. Subsamples (1 mL) of treated and control samples were taken at time 0, 90, 180, and 270 min of light exposure, serially diluted, and plated, in duplicate, in TSA medium. The dark control plates were kept in the dark immediately after plating and during the incubation period. After 24 h of dark incubation at 37 °C, the number of colonies was counted on the most convenient series of dilution. Bacterial density (CFU mL^{-1}) was determined at each time of sampling as the mean of the two duplicates. For each PS, two experiments were done and the results presented are the average of the two assays. Data are presented by survival curves plotted as logarithmic bacterial reduction in log CFU mL^{-1} *versus* light dose in J cm^{-2}.

Experimental Setup for the Photoinactivation of T4-like Phage. ***Phage Selection and Identification.*** A wastewater sample from a secondary-treated sewage plant of the city of Aveiro (Portugal) was used to select the somatic bacteriophages of *E. coli* ATCC 13706.[25] DNA extraction and purification of phage suspension were done using standard techniques.[31] The phage was identified as a T4-like phage that has 82% of homology with the *Enterobacteriaceae* phage RB43.[25] The nucleotide sequence of the phage has been deposited in the GenBank database under accession no. EU026274.

Bacteriophage Host Viability Test. As bacteria are sensible to the PS, the viability of the viral host was evaluated in order to prove that the phage inactivation was due to photoinactivation by the PS and not due to bacterial host inactivation by porphyrin. So, according to a procedure already described,[25] additional samples were collected in each sampling time after irradiation with white light. Then the samples were washed by ultracentrifugation at 28000*g* for 90 min, at room temperature, to remove the photosensitizer (washed experiments). The photosensitizer-free pellet of phages was resuspended in PBS buffer, serially diluted, and pour-plated by the double layer technique. The results obtained are identical with those resulting from direct spread (nonwashed experiments) after irradiation. This bacteriophage host viability test was done at the beginning of the work and only for the free porphyrin **2** at 5.0 μM. In the other experiments this step was not done, but the Petri dishes were incubated under dark conditions.

T4-like Phage Photoinactivation Method. A stock suspension of phages (10^9 PFU mL^{-1}, calculated by the agar double-layer technique) was diluted on phosphate buffer (PBS) until 5×10^7 PFU mL^{-1} and distributed in 600 mL acid-washed and sterilized glass beakers (20 mL of phage suspension in each beaker). After the addition of phage suspension to the beakers, hybrids **6**, **8**, and **9** were added to the respective beaker until the final concentrations of 5, 20, and 100 μM (PS concentration) were achieved. Four controls were carried out in the same conditions: dark control (MO exposed to PS without irradiation), light control (MO exposed to irradiation without PS), nonimmobilized porphyrin control (MO exposed to **2** (5 μM) under irradiation), and support control (MO exposed to nanoparticles **4** and **10** under irradiation). The beakers were then exposed to white light and subsamples (1 mL) of treated and control samples were taken at time 0, 30, 60, 90, 180, and 270 min after exposure, serially diluted and analyzed, in duplicate, for bacteriophage number by the agar double layer technique,[30] using the *E. coli* strain as host. The Petri plates were kept in the dark immediately after spread and during the incubation to avoid the inactivation of the bacterial host by the PS. Viral density (PFU mL^{-1}) was determined at each time of sampling as the mean of the two duplicates in the most convenient dilution series.[32]

For each PS, two experiments were done and the results presented are the average of the two assays. Data are presented by survival curves plotted as logarithmic phage reduction in log PFU mL^{-1} *versus* light dose in J cm^{-2}.

Acknowledgment. We are grateful to the University of Aveiro, Fundação para a Ciência e a Tecnologia (FCT) and POCI 2010 (FEDER) for funding the projects POCI/CTM/58183/2004 and PPDCT/CTM/58183/2004. C. Carvalho, E. Alves and L. Costa are also grateful to FCT for their Ph.D. grants. Thanks are also due to Nuno Micaelo for the preparation of the cover image. This work is dedicated to Prof. Carmen Nájera on the occasion of her 60th anniversary.

Supporting Information Available: Analytical and spectral characterization of the new materials and experimental work with bacteria and phages. This material is available free of charge *via* the Internet at http://pubs.acs.org.

REFERENCES AND NOTES

1. Lovell, J. F.; Liu, T. W. B.; Chen, J.; Zheng, G. Activatable Photosensitizers for Imaging and Therapy. *Chem. Rev.* **2010**, *110*, 2839–2857.
2. Plaetzer, K.; Krammer, B.; Berlanda, J.; Berr, F.; Kiesslich, T. Photophysics and Photochemistry of Photodynamic Therapy: Fundamental Aspects. *Lasers Med. Sci.* **2009**, *24*, 259–268.
3. Pandey, R. K.; Goswami, L. N.; Chen, Y.; Gryshuk, A.; Missert, J. R.; Oseroff, A.; Dougherty, T. J. Nature: A Rich Source for Developing Multifunctional Agents. Tumor-Imaging and Photodynamic Therapy. *Lasers Surg. Med.* **2006**, *38*, 445–467.
4. Carvalho, C. M. B.; Tomé, J. P. C.; Faustino, M. A. F.; Neves, M. G. P. M. S.; Tomé, A. C.; Cavaleiro, J. A. S.; Costa, L.; Alves, E.; Oliveira, A.; Cunha, Â.; *et al*. Antimicrobial Photodynamic Activity of Porphyrin Derivatives: Potential Application on Medical and Water Disinfection. *J. Porphyrins Phthalocyanines* **2009**, *13*, 574–577.
5. Cassidy, C. M.; Tunney, M. M.; McCarron, P. A.; Donnelly, R. F. Drug Delivery Strategies for Photodynamic Antimicrobial Chemotherapy: From Benchtop to Clinical Practice. *J. Photochem. Photobiol., B* **2009**, *95*, 71–80.
6. Jori, G.; Fabris, C.; Soncin, M.; Ferro, S.; Coppellotti, O.; Dei, D.; Fantetti, L.; Chiti, G.; Roncucci, G. Photodynamic Therapy in the Treatment of Microbial Infections: Basic Principles and Perspective Applications. *Lasers Surg. Med.* **2006**, *38*, 468–481.
7. Carvalho, C. M. B.; Gomes, A. T. P. C.; Fernandes, S. C. D.; Prata, A. C. B.; Almeida, M. A.; Cunha, M. A.; Tomé, J. P. C.; Faustino, M. A. F.; Neves, M. G. P. M. S.; Tomé, A. C.; *et al*. Photoinactivation of Bacteria in Wastewater by Porphyrins: Bacterial β-Galactosidase Activity and Leucine-Uptake as Methods to Monitor the Process. *J. Photochem. Photobiol., B* **2007**, *88*, 112–118.
8. Oliveira, A.; Almeida, A.; Carvalho, C. M. B.; Tomé, J. P. C.; Faustino, M. A. F.; Neves, M. G. P. M. S.; Tomé, A. C.; Cavaleiro, J. A. S.; Cunha, Â. Porphyrin Derivatives as Photosensitizers for the Inactivation of *Bacillus cereus* Endospores. *J. Appl. Microbiol.* **2009**, *106*, 1986–1995.
9. Kuznetsova, N. A.; Makarov, D. A.; Kaliya, O. L.; Vorozhtsov, G. N. Photosensitized Oxidation by Dioxygen as the Base for Drinking Water Disinfection. *J. Hazard. Mater.* **2007**, *146*, 487–491.
10. Jemli, M.; Alouini, Z.; Sabbahi, S.; Gueddari, M. Destruction of Fecal Bacteria in Wastewater by Three Photosensitizers. *J. Environ. Monit.* **2002**, *4*, 511–516.
11. Tomé, J. P. C.; Neves, M. G. P. M. S.; Tomé, A. C.; Cavaleiro, J. A. S.; Soncin, M.; Magaraggia, M.; Ferro, S.; Jori, G. Synthesis and Antibacterial Activity of New Poly-*S*-lysine-porphyrin Conjugates. *J. Med. Chem.* **2004**, *47*, 6649–6652.
12. Bonnett, R.; Krysteva, M. A.; Lalov, I. G.; Artarsky, S. V. Water Disinfection Using Photosensitizers Immobilized on Chitosan. *Water Res.* **2006**, *40*, 1269–1275.
13. Almeida, M. A.; Cavaleiro, J. A. S.; Rocha, J.; Carvalho, C. M. B.; Costa, L. A. S.; Alves, E. S. C. F.; Cunha, M. A. S. D. A.; Tomé, J. P. C.; Faustino, M. A. F.; Neves, M. G. P. M. S.; *et al*. Materiais Híbridos Nanomagnete−porfirina, Processo para a sua Síntese e Respectiva Aplicação em Desinfecção de Águas (Nanomagnet−Porphyrin Hybrid Materials: Synthesis and Water Desinfection Application). *Patent* PT 103 828.
14. Yu, C. H.; Al-Saadi, A.; Shih, S.-J.; Qiu, L.; Tam, K. Y.; Tsang, S. C. Immobilization of BSA on Silica-Coated Magnetic Iron Oxide Nanoparticle. *J. Phys. Chem. C* **2009**, *113*, 537–543.
15. Horák, D.; Babic, M.; Mackov, H.; Benes, M. J. Preparation and Properties of Magnetic Nano- and Microsized Particles

for Biological and Environmental Separations. *J. Sep. Sci.* **2007**, *30*, 1751–1772.
16. Lin, S.; Yun, D.; Qi, D. W.; Deng, C. H.; Li, Y.; Zhang, X. M. Novel Microwave-Assisted Digestion by Trypsin-Immobilized Magnetic Nanoparticles for Proteomic Analysis. *J. Proteome Res.* **2008**, *7*, 1297–1307.
17. Gao, L. Z.; Wu, J. M.; Lyle, S.; Zehr, K.; Cao, L. L.; Gao, D. Magnetite Nanoparticle-Linked Immunosorbent Assay. *J. Phys. Chem. C* **2008**, *112*, 17357–17361.
18. Park, M. E.; Chang, J. H. High Throughput Human DNA Purification with Aminosilanes Tailored Silica-Coated Magnetic Nanoparticles. *Mater. Sci. Eng., C* **2007**, *27*, 1232–1235.
19. Gu, H. W.; Xu, K. M.; Yang, Z. M.; Chang, C. K.; Xu, B. Synthesis and Cellular Uptake of Porphyrin Decorated Iron Oxide Nanoparticles—A Potential Candidate for Bimodal Anticancer Therapy. *Chem. Commun.* **2005**, 4270–4272.
20. McCarthy, J. R.; Weissleder, R. Multifunctional Magnetic Nanoparticles for Targeted Imaging and Therapy. *Adv. Drug Delivery Rev.* **2008**, *60*, 1241–1251.
21. Quarta, A.; Di Corato, R.; Manna, L.; Ragusa, A.; Pellegrino, T. Fluorescent-Magnetic Hybrid Nanostructures: Preparation, Properties, and Applications in Biology. *IEEE Trans. Nanobiosci.* **2007**, *6*, 298–308.
22. Liu, X.; Ma, Z.; Xing, J.; Liu, H. Preparation and Characterization of Amino-Silane Modified Superparamagnetic Silica Nanospheres. *J. Magn. Magn. Mater.* **2004**, *270*, 1–6.
23. Maestrin, A. P. J.; Ribeiro, A. O.; Tedesco, A. C.; Neri, C. R.; Vinhado, F. S.; Serra, O. A.; Martins, P. R.; Iamamoto, Y.; Silva, A. M. G.; Tomé, A. C.; *et al*. A Novel Chlorin Derivative of Meso-tris(pentafluorophenyl)-4-pyridylporphyrin: Synthesis, Photophysics and Photochemical Properties. *J. Braz. Chem. Soc.* **2004**, *15*, 923–930.
24. Alves, E.; Costa, L.; Carvalho, C.; Tome, J.; Faustino, M.; Neves, M.; Tome, A.; Cavaleiro, J.; Cunha, A.; Almeida, A. Charge Effect on the Photoinactivation of Gram-Negative and Gram-Positive Bacteria by Cationic Meso-substituted Porphyrins. *BMC Microbiol.* **2009**, *9*, 70–83.
25. Costa, L.; Alves, E.; Carvalho, C. M. B.; Tomé, J. P. C.; Faustino, M. A. F.; Neves, M. G. P. M. S.; Tomé, A. C.; Cavaleiro, J. A. S.; Cunha, Â.; Almeida, A. Sewage Bacteriophage Photoinactivation by Cationic Porphyrins: A Study of Charge Effect. *Photochem. Photobiol. Sci.* **2008**, *7*, 415–422.
26. Alves, E.; Carvalho, C. M. B.; Tomé, J. P. C.; Faustino, M. A. F.; Neves, M. G. P. M. S.; Tomé, A. C.; Cavaleiro, J. A. S.; Cunha, A.; Mendo, S.; Almeida, A. Photodynamic Inactivation of Recombinant Bioluminescent *Escherichia coli* by Cationic Porphyrins under Artificial and Solar Irradiation. *J. Ind. Microbiol. Biotechnol.* **2008**, *35*, 1447–1454.
27. Tavares, A.; Carvalho, C. M. B.; Faustino, M. A.; Neves, M. G. P. M. S.; Tomé, J. P. C.; Tomé, A. C.; Cavaleiro, J. A. S.; Cunha, Â.; Gomes, N. C. M.; Alves, E.; Almeida, A. Antimicrobial Photodynamic Therapy: Study of Bacterial Recovery Viability and Potential Development of Resistance after Treatment. *Mar. Drugs* **2010**, *8*, 91–105.
28. Guinier, A. *X-ray Diffraction*; Freeman: San Francisco, 1963.
29. Costa, L.; Carvalho, C. M. B.; Faustino, M. A. F.; Neves, M. G. P. M. S.; Tomé, J. P. C.; Tomé, A. C.; Cavaleiro, J. A: S.; Cunha, Â.; Almeida, A. Sewage Bacteriophage Inactivation by Cationic Porphyrins: Influence of Light Parameters. *Photochem. Photobiol. Sci.* **2010**, *9*, 1126–1133.
30. Adams, M. H. *Bacteriophages*; Interscience Publishers, Inc.: New York, 1959; pp 91−92.
31. Sambrook, J.; Fritsch, E.; Maniatis, T., Bacteriophage ë and Its Vectors: Extraction of bacteriophage λ DNA. In *Molecular Cloning: A Laboratory Manual*, 2nd ed.; Sambrook, J., Russel, D. W., Eds.; Cold Spring Harbor Laboratory Press: New York, 1989; pp 2.80−2.81.
32. Costa, L. Sewage Bacteriophage Photoinactivation by Free and Immobilized Porphyrins. MSc Thesis, 2007, University of Aveiro, Portugal.